Title	Fragmentation processes of C-60 in multiple electron loss and capture collisions of 2-MeV Si2+
Author(s)	Majima, T; Nakai, Y; Mizuno, T; Tsuchida, H; Itoh, A
Citation	PHYSICAL REVIEW A (2006), 74(3)
Issue Date	2006-09
URL	http://hdl.handle.net/2433/50081
Right	Copyright 2006 American Physical Society
Type	Journal Article
Textversion	publisher; none

Fragmentation processes of C_{60} in multiple electron loss and capture collisions of 2-MeV Si^{2+}

T. Majima,[1,*] Y. Nakai,[2] T. Mizuno,[1] H. Tsuchida,[1] and A. Itoh[1]
[1]*Quantum Science and Engineering Center, Kyoto University, Kyoto 606-8501, Japan*
[2]*RIKEN (The Institute of Physical and Chemical Research), Wako, Saitama 351-0198, Japan*
(Received 4 June 2006; published 18 September 2006)

An experimental study of ionization and fragmentation of C_{60} has been performed for 2-MeV Si^{2+} incident ions under charge-changing conditions. Time-of-flight (TOF) spectra of product ions and number distributions of secondary electrons (n_e) were measured in coincidence with charge-selected outgoing projectiles. TOF spectra from transiently formed highly charged C_{60}^{r+} ions are obtained for individual charge states r, and n_e distributions correlated with size-fixed C_m^+ ions are also obtained for $m<15$. It is found that mass spectra and n_e distributions are both significantly different between loss and capture collisions, whereas a remarkable similarity in the partial n_e distributions is observed almost independently of the different charge-changing conditions when compared at given C_m^+ ions size. We find also that a number of secondary electrons as high as 20 are emitted in the production of small fragment ions. Furthermore, small fragment ions are produced predominantly in close collisions even at very low charge states of $r \simeq 3$ in comparison with distant collisions. This indicates that the energy partition rate between ionization and internal excitation might be considerably different in close and distant collisions.

DOI: 10.1103/PhysRevA.74.033201 PACS number(s): 36.40.Qv, 34.50.Gb, 61.48.+c

I. INTRODUCTION

In the last decade, considerable effort has been devoted to study of collision-induced ionization and fragmentation of C_{60} to achieve microscopic understanding of excitation and relaxation mechanisms involving polyatomic molecules and clusters (see [1] and references therein). The remarkable high stability against Coulomb explosion is one of the outstanding properties of C_{60} and has been verified in several different experiments using electron impact [2], slow highly charged ion (SHCI) impact [3–6], and strong laser fields [7]. The charge state of intact C_{60}^{r+} ions observed in these investigations reaches up to $r \sim 9$ with lifetimes of the order of microseconds. In addition, remarkably high charge states of fullerene ions as high as $r=12$ were observed in recent experimental work using an intense femtosecond laser [8]. On the other hand, small-sized fragment ions resulting from multifragmentation processes are, by and large, observed in fast heavy-ion collisions [9–15]. Moreover, we found recently that multifragmentation occurs at very low charge states of $r \sim 3$ in 2-MeV Si^{2+} collisions when measured in coincidence with single-electron loss and capture collision events [16].

The experimental findings described above indicate clearly that the stability of a highly charged C_{60}^{r+} ion is basically dependent on its charge state r but also affected significantly by the amount of its internal excitation energy after interactions. This is because the internal excitation energy, denoted by E_{int} hereafter, is expected to be greatly different in the different kinds of experiments described above. Actually, E_{int} of a highly charged C_{60}^{12+} ion produced by a laser is estimated to be only 15 eV [8]. Also, in SHCI collisions, E_{int} is supposed to be small because the predominant production mechanism of highly charged C_{60}^{r+} ions is multiple-electron capture taking place in distant collisions [3,5]. By contrast, electron loss and capture collisions of fast heavy ions are rather close-encounter processes and, consequently, a much larger amount of E_{int} can be deposited into the molecule even if its charge state r is very small as observed experimentally [16]. It is, therefore, important to know to what extent the fragmentation pattern is affected by the charge state and the internal excitation in fast ion collisions.

Campbell *et al.* [17] measured fragment ion distributions by using a femtosecond laser. They observed the fragmentation pattern to change from the ionization regime (r) to the internal excitation regime (E_{int}) as a function of the laser pulse duration ranging from 25 fs to 5 ps. Unlike laser experiments of this kind, however, ionization and excitation by energetic heavy-ion impact are essentially simultaneous processes and will appear in widely different manners according to a variety of combinations among projectile species, incident energy, and charge state. For the purpose of close inspection of these dynamical behaviors of C_{60} fragmentation, a triple-coincidence technique [5,16] serves as a powerful tool, allowing us to obtain three kinds of information simultaneously about fragment ion distributions, number distributions of secondary electrons, and outgoing charge states of projectile particles. Actually, we found evidence for the predominant importance of internal excitation over the apparent charge state r in single-electron loss and capture collisions of 2-MeV Si^{2+} ions [16]. In that paper we pointed out that the number of free electrons (n_i) emitted from a C_{60} molecule is in practice very important to examine the degree of C_{60} fragmentation because the value of n_i is closely related to the amount of E_{int}.

In this work, we extended measurements to multiple-electron loss and capture collisions, in which r and E_{int} are both expected to be considerably large compared with single-electron processes. It is emphasized that the present triple-

*Permanent address: East Tokyo Laboratory, Genesis Research Institute, Inc., 717-86 Futamata, Ichikawa, Chiba 272-0001, Japan.

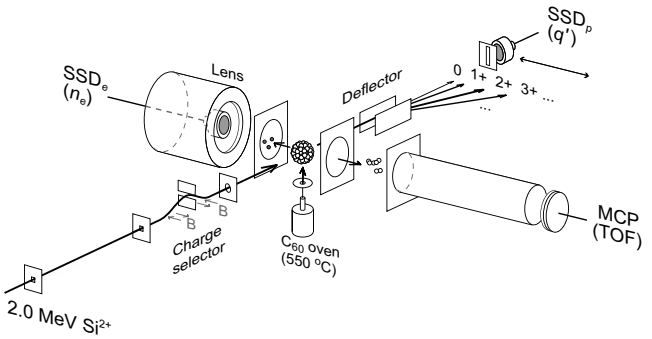

FIG. 1. Schematic of experimental setup of the TOF n_e coincidence measurements.

coincidence method provides information systematically about fragmentation profiles according to individual values of n_i and r, enabling us to ascertain the relative significance of r and E_{int} in C_{60} multifragmentation.

II. EXPERIMENT

The experiment was performed at the QSEC tandem accelerator facility of Kyoto University. A schematic diagram of the experiment is shown in Fig. 1. A beam of 2-MeV Si^{2+} extracted from the accelerator was collimated to about 0.2×0.5 mm^2 with two sets of four-jaw slits. Impurity ions of undesirable charge states produced in collisions with residual gases were removed by a charge selector consisting of four magnetic deflectors located just before a crossed-beam collision chamber. The charge-selected beam then crossed an effusive molecular beam target of C_{60} in the collision chamber. A base pressure of the chamber was below 1×10^{-6} Pa. The C_{60} target was produced by sublimation of high-purity (99.98%) powder at 550 °C in a quartz oven with an exit nozzle of 2 mm in diameter. The C_{60} beam was collimated by a thin aperture of 1 mm in diameter at 10 mm below the projectile beam axis. The diameter of the C_{60} beam in a collision region was estimated to be smaller than 4 mm which was small enough to detect nearly all the product ions and secondary electrons.

Fragment ions as well as intact ions produced in collisions were extracted by an electrostatic field of 615 V/cm perpendicular to both the incident beam and the C_{60} beam, and were detected by a two-stage multichannel-plate (MCP) detector with a front voltage of −4.6 kV. The mass-to-charge ratio of product ions was measured with a time-of-flight (TOF) spectrometer operated under Wiley-McLaren spatial-focusing conditions [18]. Secondary electrons were extracted in the opposite direction to the positive ions and collected by a focusing lens into a semiconductor solid-state detector (SSD$_e$) with an active area of 150 mm^2. A positive voltage of 30 kV was applied on the detector. Hence, the pulse heights of signals from the SSD$_e$ are proportional to the total energy ($30n_e$ keV) of electrons when n_e electrons are detected simultaneously. The pulse height distribution provides, therefore, the number distribution of secondary electrons.

Outgoing projectile particles of Si^{q+} were charge separated by an electrostatic deflector and detected by a movable solid-state detector (SSD$_p$) which had a rectangular entrance slit of 0.5 mm (horizontal) × 5 mm (vertical). The corresponding acceptance angles for scattered particles were ±0.4 mrad (horizontal) and ±4 mrad (vertical), respectively. Measurements were made at two SSD$_p$ positions in the horizontal direction, corresponding to scattering angles of $\theta=0$ and 0.8 mrad, respectively. This is because charge-changing collisions involving multiple electrons are supposed to take place at small impact parameters resulting in noticeable deflection of incident particles. Comparison between different scattering angles is, therefore, important to achieve a closer inspection of the TOF spectra. An example is shown in Fig. 2 obtained for two-electron-loss collisions. Obviously, two spectra are completely different and, in particular, only small fragment ions are produced at $\theta=0.8$ mrad. These angular-dependent TOF spectra will be discussed later.

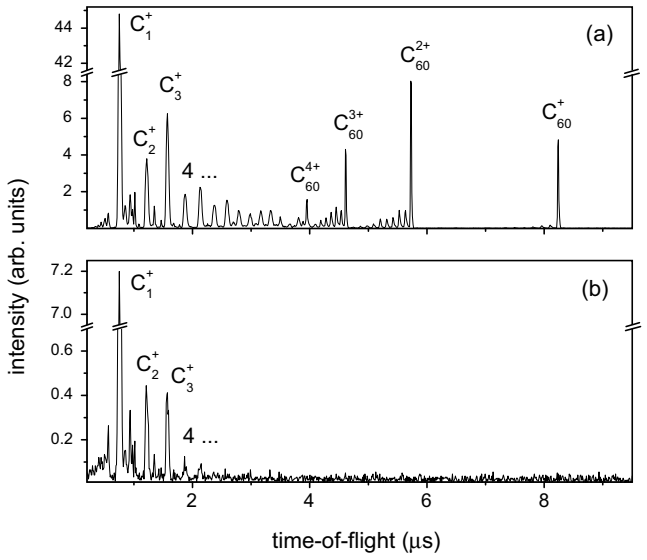

FIG. 2. Comparison of TOF spectra for $2e$ loss collisions measured at two scattering angles: (a) $\theta=0\pm0.4$ mrad and (b) 0.8 ± 0.4 mrad.

Triple-coincidence measurements of TOF spectra and n_e distributions at fixed final charge states q were performed by using the SSD$_p$ signals as start triggers. We investigated one- and two-electron capture ($q=0,1$) collisions and one- through three-electron loss ($q=3-5$) collisions. Data were recorded two-dimensionally in 1024×1024 channels for each charge-changing condition. Symbols used in this paper are as follows: r is the charge state of a prefragmented ion C_{60}^{r+}, n_e is the number of electrons detected by the SSD$_e$, n_i is the number of free electrons emitted from C_{60}, referred to as pure-ionization, n_c is the number of electrons captured by a projectile, and n_l is the number of electrons lost from a projectile.

Also, the following relationships hold:

$$n_e = n_i, \quad r = n_i + n_c = n_e + n_c \quad \text{for electron capture}, \tag{1}$$

$$n_e = n_i + n_l, \quad r = n_i = n_e - n_l \quad \text{for electron loss}. \tag{2}$$

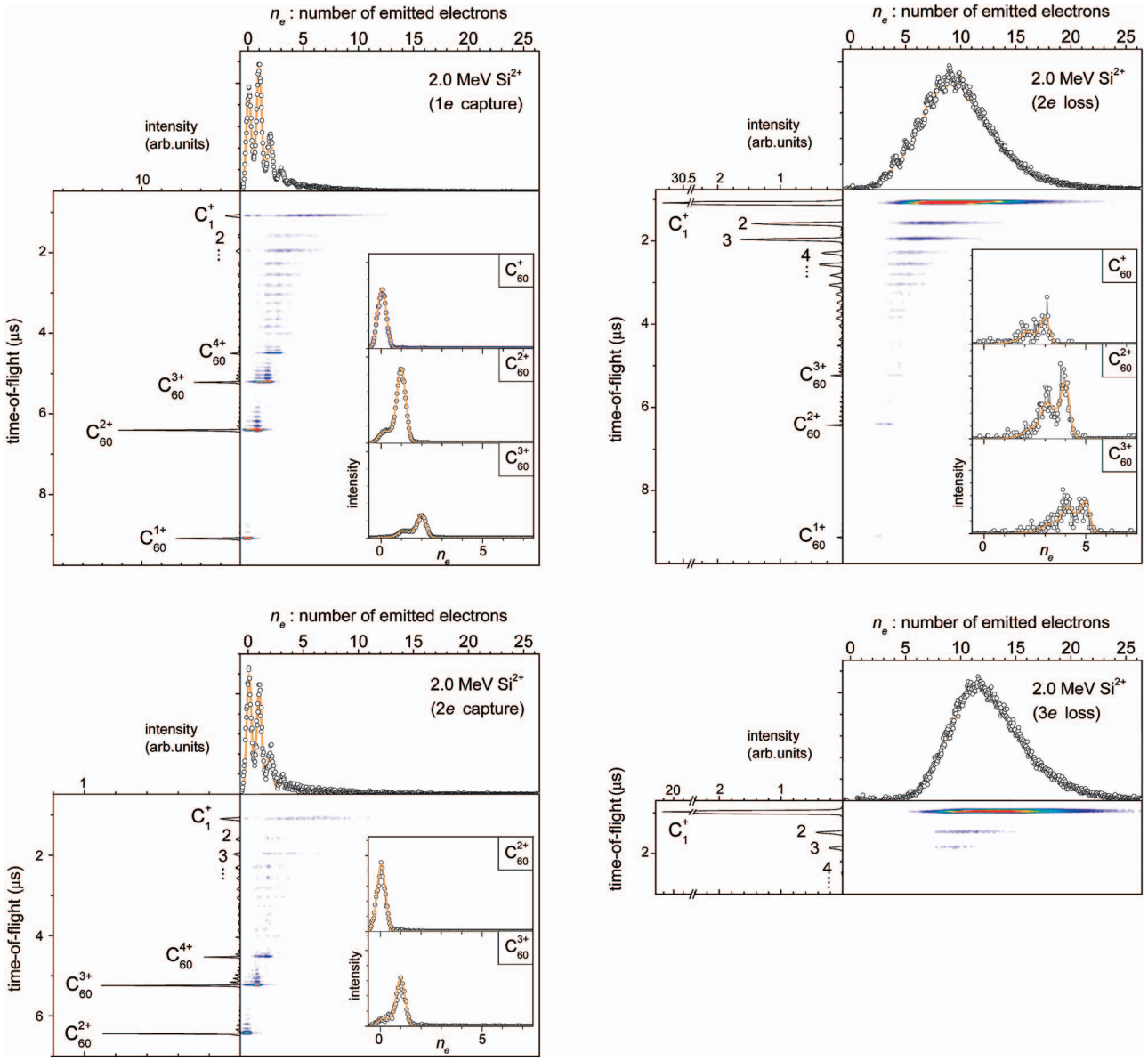

FIG. 3. (Color) Two-dimensional coincidence maps of TOF and n_e spectra obtained for various charge-changing collisions as noted; $1e,2e$ capture collisions ($Si^{2+}\rightarrow Si^{+},Si^{0}$) and $2e,3e$ loss collisions ($Si^{2+}\rightarrow Si^{4+},Si^{5+}$). Insets show n_e spectra correlated with intact parent ions $C_{60}{}^{r+}$.

III. EXPERIMENTAL RESULTS

Figure 3 shows four examples of two-dimensional coincidence maps obtained for various charge-changing collisions. The vertical and horizontal axes represent, respectively, the mass-to-charge ratio of product ions and the pulse height of SSD_e signals, which corresponds to the number of secondary electrons n_e emitted simultaneously. An n_e distribution correlated with a given size of product ion is obtained from the data points lined up horizontally at the position of the corresponding TOF and will be called the partial n_e spectrum hereafter. Similarly, a partial time-of-flight spectrum correlated with the emission of n_e electrons is obtained from the data points lined up vertically at a position of n_e. A series of partial TOF spectra associated with fixed charge states r of prefragmented $C_{60}{}^{r+}$ ions were derived by using Eqs. (1) and (2). Total n_e distributions and total TOF spectra are obtained by projecting all these data points onto the two axes, respectively, as demonstrated in the figures.

The insets show the partial n_e spectra correlated with intact parent ions of $C_{60}{}^{r+}$ ($r=1-3$). As described in our previous paper [16], analysis of these partial spectra of parent ions provides the electron-detection efficiency of the SSD_e detector. This is because the value of n_e is uniquely determined from Eqs. (1) and (2) if all the emitted electrons as well as intact $C_{60}{}^{r+}$ ions are detected safely. As shown by solid lines, all the n_e spectra can be reproduced almost perfectly by using fitting parameters of 0.17 as the backscattering probability and 0.6 as the backscattering K factor [16,19]. The electron-detection efficiency obtained in this way was 0.94, implying that nearly all the secondary electrons including also fast electrons (~39 eV) lost from a pro-

jectile ion are detected successfully in the present experiment. It is noted that all the partial n_e distributions used hereafter were deduced precisely by this fitting calculation carried out with the same fitting parameters mentioned above.

Overall features derived from Fig. 3 are as follows. First, the total TOF spectra are significantly different between loss and capture collisions. The dominant products are small-sized fragment ions in loss collisions but intact C_{60}^{r+} ions in capture collisions. In electron loss collisions, yields of small fragment ions C_m^+ ($m \leqslant 3$) were found to increase rapidly with increasing number of n_l. For instance, in collisions of $3e$ loss from $Si^{2+}(2p^6 3s^2)$ to $Si^{5+}(2p^5)$, the spectrum is completely dominated by the smallest fragments of $m \leqslant 3$ and exhibits no intact C_{60}^{r+} ions, which are still visible in $1e$ and $2e$ loss collisions. This implies certainly that, compared to the outer-shell ionization of $3s$ electrons, additional $2p$ ionization induces a larger amount of energy deposition, resulting in nearly complete cage disintegration. Unlike for loss collisions, spectra for $1e$ and $2e$ capture collisions do not show a noticeable difference in the TOF spectra except for intact parent ions.

Second, the total n_e spectra exhibit also strong dependence on the charge-changing condition. The spectra for electron loss collisions show clearly a large number of electrons as high as 20 to be emitted, whereas only a few electrons in capture collisions. More detailed comparisons between loss and capture collisions are shown in Fig. 4, where total and partial distributions are plotted as a function of the charge state r of prefragmented C_{60}^{r+} ions. The distributions show roughly double-peak structures attributable to intact C_{60}^{r+} ions and small fragment C_m^+ ions. The main reason for this capture-loss difference in distribution shape is due to the difference in relative magnitude between these two components. Obviously the former component is confined to smaller values of r compared to the latter which reveals much larger r and broader peak profiles. One can see, therefore, that electron capture collisions, where intact ions are produced preferentially, are soft or distant collisions resulting in low charge states of intact ions. On the other hand, in electron loss collisions the latter component contributes predominantly, particularly for $n_l \geqslant 2$.

Despite considerable broadness of distribution profiles, it is helpful to examine mean charge states $\bar{r}$ for obtaining an overall picture of ionization and fragmentation. From the data of total n_e distributions the values of $\bar{r}$ were obtained as $\bar{r} \simeq n_c + 1.7$ ($n_c = 1, 2$) for capture and $\bar{r} \simeq 3.2 n_l + 3.8$ ($n_l = 1-3$) for loss collisions. Hence, in loss collisions about 3.2 electrons are released additionally from C_{60} per each electron loss event, while no such additional ionization occurs in capture events. Using Eqs. (1) and (2), the average number of pure ionization events, n_i, can also be derived as $\bar{n}_i = \bar{r} - n_c \simeq 1.7$ for capture and $\bar{n}_i = \bar{r} = 3.2 n_l + 3.8$ for loss collisions. It is pointed out that n_i is supposed to be correlated closely with the amount of electronic energy deposition E_d [11,16], and once the impact parameter is given, both n_i and E_d may be determined. In this sense, the present result of completely different n_e distributions indicates that a specific charge-changing collision takes place preferentially in a specific impact parameter region. Therefore, the result of $n_i \simeq 1.7$ obtained for $1e$ and $2e$ capture collisions implies that both processes occur at nearly equivalent impact parameters,

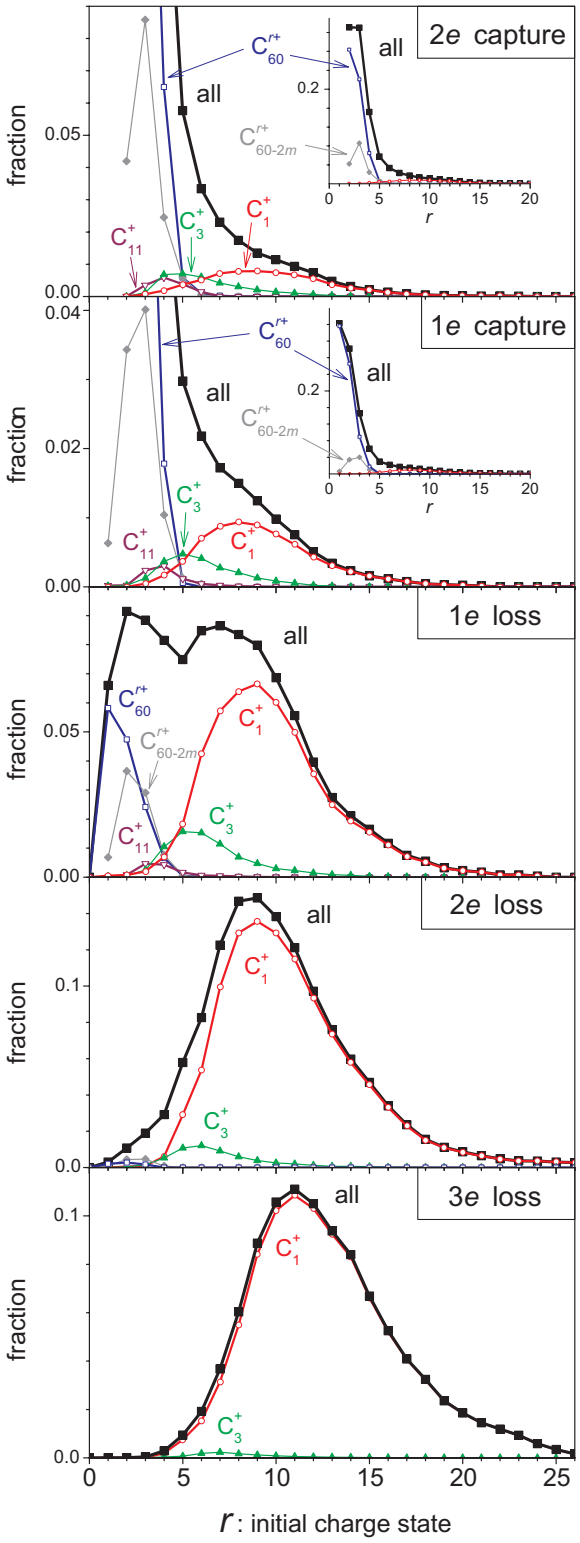

FIG. 4. (Color) Total and partial distributions of secondary electrons as a function of the charge state r of prefragmented C_{60}^{r+} ions obtained in various electron capture and loss collisions.

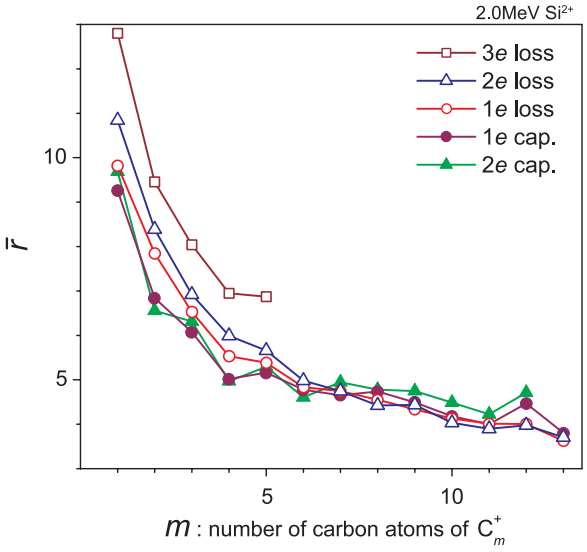

FIG. 5. (Color) Mean charges associated with C_m^+ as a function of the cluster size m obtained for charge-changing collisions.

while in loss collisions the impact parameter becomes smaller with increasing n_l.

In contrast to the total distributions, the partial n_e distribution correlated with a specific fragment ion reveals surprisingly little dependence on the collision condition. As a typical example, the distribution profile correlated with C_1^+ is found to peak at nearly the same position of $r=8-11$ for all the collision processes including even capture events. The characteristics of this independency are demonstrated more clearly in Fig. 5 by plotting $\bar{r}$ as a function of the cluster size m of C_m^+ $(m=1-13)$. One can see $\bar{r}$ at the same m to be essentially equivalent for all the collision processes except for $3e$ loss, for which the value is about 20% higher than others. It is interesting to note that the overall dependence on the size m can roughly be expressed as $\bar{r}=(11\pm1)\times\exp(-m/10)$ except for $3e$ loss events. Consequently, it is plausible to state that a fragment ion of fixed m may be produced in equivalent impact parameter collisions independently of the charge-changing condition. This leads us again to the conclusion that E_d is almost equivalent in the production of size-fixed fragment ions. Otherwise it is hard to explain such a high degree of multiple ionization as observed in single-capture collisions. However, one should be reminded from Fig. 4 that violent collisions leading to multifragmentation are very minor events, accounting for at most only a few percent of the total capture events; see the relative intensities of C_1^+ in the top two figures where contributions from intact ions are predominant.

IV. DISCUSSION

We discuss here in more detail the relative importance of the charge state r of prefragmented parent ions and internal excitation. First, the intensities of product ions measured for multiple charge-changing collisions are examined in terms of the number of pure ionization events n_i. This is based on the idea that the total energy deposition E_d is shared by ionization (n_i) and internal excitation (E_{int}) with a certain partition rate, and therefore the value of n_i is regarded as a good measure of the amount of E_{int}. For convenience, product ions are divided into three groups of parent ions including large daughter ions $(\Sigma_{m=0}^{5}C_{60-2m}^{r+})$, medium sized ions $(\Sigma_{m=4}^{15}C_m^+)$ and the smallest three fragments $(\Sigma_{m=1}^{3}C_m^+)$. The relative intensities of these product ions are denoted by R_p, R_m, and R_s,

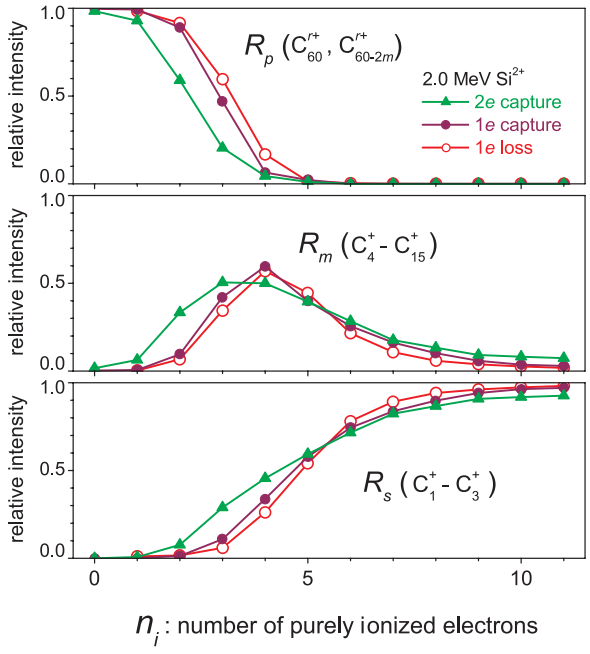

FIG. 6. (Color) Relative intensities of fullerenelike ions (R_p), medium-sized fragments (R_m), and small-sized fragments (R_s) obtained for electron capture collisions. Data of $1e$ loss are drawn for comparison.

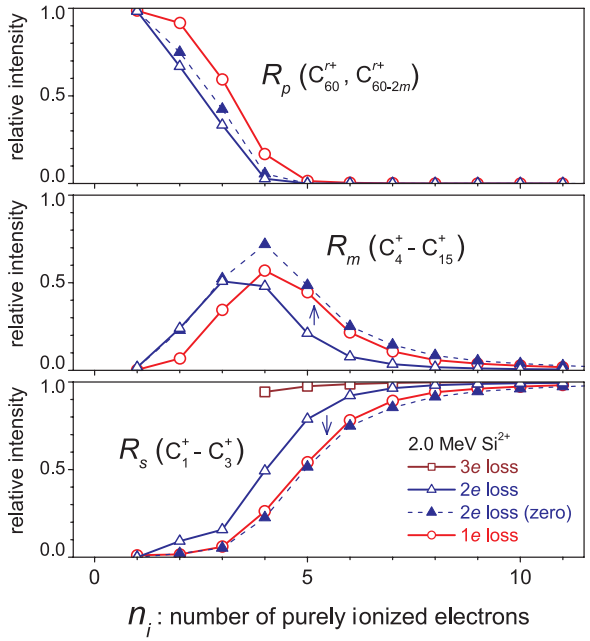

FIG. 7. (Color) As in Fig. 6, obtained for electron loss collisions.

respectively, with a relationship of $R_p+R_m+R_s=1$. Results for electron capture and loss collisions are shown in Figs. 6 and 7, respectively, where data of $1e$ loss are plotted in both figures for comparison. These figures show clearly that multifragmentation is always dominant at $n_i>8$ for all the collision processes (see also Fig. 4). This implies evidently that the Coulomb repulsion force and internal excitation are both high enough to induce multifragmentation in such violent collisions. Since $R_s \simeq 1$ in this region, the following discussion is focused on the region of $n_i<8$.

At $n_i<5$ in Fig. 6, fragmentation yields (R_m and R_s) in $2e$ capture collisions are slightly enhanced. This indicates that the instability due to Coulomb repulsion becomes more important in the fragmentation of low-charged C_{60}^{r+} ions in comparison with E_{int}. At $n_i=4$, for instance, the charge states r for $1e$ loss, $1e$ capture, and $2e$ capture collisions are 4, 5, and 6, respectively, and corresponding total Coulomb potentials V_c (eV) are known from [2,20] to be 15.10 ($r=4$), 26.64 ($r=5$), and 41.08 ($r=6$). On the other hand, E_{int} is estimated from a statistical partitioning model to be 53 eV at $n_i=4$ as described in [16]. If we consider the sum of V_c and E_{int} as the total "instability energy," we obtain 68.1, 79.6, and 94.1 eV for $r=4$, 5, and 6, respectively. Here, it is worth noting the theoretical results of maximum entropy calculations made for a neutral C_{60} by Campbell *et al.* [21]. They showed that the multifragmentation starts at $E_{int} \simeq 85$ eV and entire destruction into small fragments occurs beyond 225 eV, whereas the molecule keeps its fullerene structure below 85 eV. Hence, in a qualitative sense, our instability energy seems to explain reasonably the enhancement of multifragmentation at $n_i<5$ in $2e$ capture collisions. It should be noted that the instability due to Coulomb explosion is the predominant fragmentation mechanism in SHCI collisions, where the main process of C_{60}^{r+} production is distant electron capture collisions accompanying small internal excitation energies [5]

In electron loss collisions (Fig. 7), there are some discrepancies in fragmentation yields at $n_i<8$. For instance, at $n_i=5$, the values of R_s are 0.50, 0.76, and 0.98 for $n_l=1$, 2, and 3, respectively. These results are in contrast to our energy partitioning model, because both the internal energy and charge states are supposed to be constant at a fixed value of n_i, irrespective of n_ℓ, in electron loss collisions. However, our experimental results indicate that the internal energy at the same n_i becomes higher with increasing n_ℓ.

Similar behaviors are observed more directly in the scattering angle dependence of loss collisions. As we saw already in Fig. 2, TOF spectra are completely different for zero-degree and off-center angles. By taking account of the geometry of our detection system, zero-degree and scattering components were deduced separately as plotted in Fig. 8 with blank bars ($\theta=0$) and solid bars ($\theta=0.8$ mrad), respectively. One can see that, even at low charge states r ($=n_i$), small fragment ions are predominantly produced in off-center scatterings. Consequently, these components lead to enhancement of multifragmentation shown in Fig. 7. Actually, experimental values of R_s for $2e$ loss collisions become identical with those for $1e$ loss collisions after subtracting the scattering components as depicted by arrows in Fig. 7.

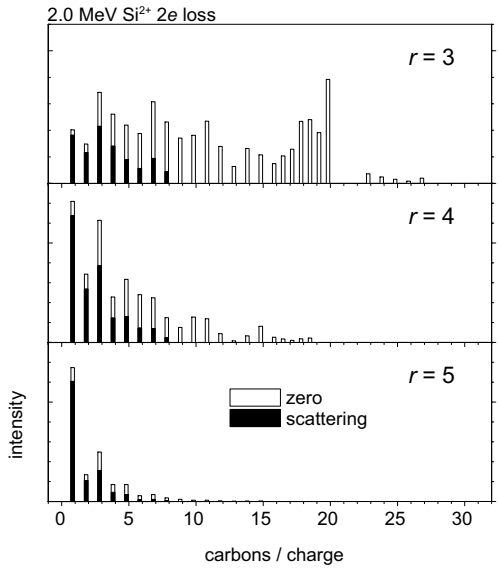

FIG. 8. Comparison of intensity distributions of product ions between zero-degree components (blank bars) and scattering components (solid bars) deduced by taking account of our detector geometry.

We note here that scattering components were negligibly small for $1e$ loss and capture collisions ($n_c=1,2$) but predominantly large for $3e$ loss collisions. These results indicate that the impact parameter becomes smaller as n_ℓ increases in loss collisions.

Enhanced multifragmentation observed at nonzero scattering angles implies evidently that the internal excitation energy is higher than small-angle scattering when compared at the same n_i ($=r$). Note that the recoiling effect of a target carbon atom is also ruled out from consideration because the recoil energy is estimated to be only 6.7 eV at most ($\theta=1.2$ mrad) in a collision of Si+C. The present results indicate that the partition rate in close collisions may be considerably different from that in distant collisions; namely, close collisions are supposed to induce internal excitation greatly in comparison with distant collisions, whereas the degree of pure ionization is the same in both collisions.

As another explanation, we speculate that the energy partitioning rate itself has a certain statistical width around the mean value. It might, therefore, be possible to result in relatively larger E_{int} but smaller n_i than expected from the mean partition rate, leading to a higher degree of multifragmentation at small n_i's. The present results of enhanced fragmentation in $2e$ and $3e$ loss collisions at $n_i<8$ seem to reflect this statistical nature of the energy partitioning process.

V. SUMMARY

The correlated processes of fragmentation and ionization of C_{60} induced in charge-changing collisions of 2-MeV Si^{2+} have been investigated in detail by specifying the charge state of prefragmented C_{60}^{r+} ions and the number of free electrons (n_e) emitted simultaneously from both target and incident particles. Some important findings are listed below.

First, a huge number of secondary electrons as high as 20 are emitted in the production of small fragment ions like C_1^+ and these n_e distributions exhibit nearly the same shape in all the charge-changing conditions including also $1e$ capture events. Second, multiple-electron loss collisions ($n_l \geqslant 2$) take place predominantly at smaller impact parameters, resulting in the deflection of incident ion trajectories and the corresponding TOF spectra are dominated by only the few smallest fragment ions. By contrast, electron capture of both $1e$ and $2e$ is a distant-collision process without accompanying noticeable deflection of incident ions.

The present results are examined with an energy partition model stating that the internal excitation energy E_{int} may possibly be estimated from a certain partition rate once r and n_e are known simultaneously. With this model, various fragmentation phenomena, which are significantly different in different charge-changing conditions, are successfully analyzed in terms of the degree of pure ionization n_i of a target molecule. Although the C_{60} fragmentation is induced mainly via internal excitation, the instability due to Coulomb repulsive force is found to become also important at $n_i \leqslant 4$ for electron capture collisions. As for the region of large values of n_i (>8), it is concluded that the C_{60} fragmentation is induced via both internal excitation and the Coulomb repulsion force, irrespective of electron capture and loss collisions.

Finally, the predominant multifragmentation observed at nonzero scattering angles implies that the partition rate may be considerably different in close and distant collisions. It is, therefore, important to know the impact-parameter-dependent partition rate to achieve further detailed understanding of the fragmentation mechanisms.

ACKNOWLEDGMENT

One of the authors (T.M.) would like to acknowledge support by a Grant-in-Aid from JSPS. We also acknowledge K. Yoshida, K. Norizawa, and M. Naitoh for their technical support during the experiment.

[1] E. E. B. Campbell and F. Rohmund, Rep. Prog. Phys. **63**, 1061 (2000).
[2] P. Scheier and T. D. Märk, Phys. Rev. Lett. **73**, 54 (1994).
[3] B. Walch, C. L. Cocke, R. Voelpel, and E. Salzborn, Phys. Rev. Lett. **72**, 1439 (1994).
[4] J. Jin, H. Khemliche, M. H. Prior, and Z. Xie, Phys. Rev. A **53**, 615 (1996).
[5] S. Martin, L. Chen, A. Denis, R. Bredy, J. Bernard, and J. Désesquelles, Phys. Rev. A **62**, 022707 (2000).
[6] S. Tomita, H. Lebius, A. Brenac, F. Chandezon, and B. A. Huber, Phys. Rev. A **67**, 063204 (2003).
[7] E. E. B. Campbell, K. Hoffmann, H. Rottke, and I. V. Hertel, J. Chem. Phys. **114**, 1716 (2001).
[8] V. R. Bhardwaj, P. B. Corkum, and D. M. Rayner, Phys. Rev. Lett. **91**, 203004 (2003).
[9] Y. Nakai, A. Itoh, T. Kambara, Y. Bitoh, and Y. Awaya, J. Phys. B **30**, 3049 (1997).
[10] A. Reinköster, U. Werner, and H. O. Lutz, Europhys. Lett. **43**, 653 (1998).
[11] H. Tsuchida, A. Itoh, K. Miyabe, Y. Bitoh, and N. Imanishi, J. Phys. B **32**, 5289 (1999).
[12] T. Schlathölter, O. Hadjar, R. Hoekstra, and R. Morgenstern, Phys. Rev. Lett. **82**, 73 (1999).
[13] O. Hadjar, P. Földi, R. Hoekstra, R. Morgenstern, and T. Schlathölter, Phys. Rev. Lett. **84**, 4076 (2000).
[14] A. Itoh, H. Tsuchida, K. Miyabe, T. Majima, and Y. Nakai, Phys. Rev. A **64**, 032702 (2001).
[15] D. Bordenve-Montesquieu, P. Moretto-Capelle, A. Bordenave-Montesquieu, and A. Rentenier, J. Phys. B **34**, L137 (2001).
[16] T. Majima, Y. Nakai, H. Tsuchida, and A. Itoh, Phys. Rev. A **69**, 031202(R) (2004).
[17] E. E. B. Campbell, K. Hansen, K. Hoffmann, G. Korn, M. Tchaplyguine, M. Wittmann, and I. V. Hertel, Phys. Rev. Lett. **84**, 2128 (2000).
[18] W. C. Wiley and I. H. McLaren, Rev. Sci. Instrum. **26**, 1150 (1955).
[19] G. Lakits, F. Aumayr, and H. Winter, Rev. Sci. Instrum. **60**, 3151 (1989).
[20] S. Petrie, J. Wang, and D. K. Bohme, Chem. Phys. Lett. **204**, 473 (1993).
[21] E. E. B. Campbell, T. Raz, and R. D. Levine, Chem. Phys. Lett. **253**, 261 (1996).